Raman study of the structural phase transition in the ordered perovskite Pb_2MgWO_6

1995 J. Phys.: Condens. Matter 7 8109

(http://iopscience.iop.org/0953-8984/7/42/008)

J. Phys.: Condens. Matter 7 (1995) 8109–8117. Printed in the UK

Raman study of the structural phase transition in the ordered perovskite Pb_2MgWO_6

G Baldinozzi†§, Ph Sciau† and A Bulou‡

† Laboratoire de Chimie Physique du Solide, URA CNRS 453, Ecole Centrale Paris, F-92295 Châtenay-Malabry Cédex, France

‡ Laboratoire de Physique de l'Etat Condensé, URA CNRS 807, Université du Maine, F-72017 Le Mans Cédex, France

Received 1 June 1995

Abstract. Lead magnesium tungstate Pb_2MgWO_6 undergoes a structural phase transition at about 310 K. This phase transition has been characterized by Raman spectroscopy. The main features of the Raman spectra, collected between 173 and 523 K, are consistent with group theoretical predictions though unexpected weak and broad signals are observed in the high-temperature phase. From the comparison between these results and the structures previously determined, it is concluded that the phase transition has a behaviour intermediate between pure displacive and order–disorder.

1. Introduction

The highly ordered perovskite-like Pb_2MgWO_6 actually belongs to the elpasolite structure. It undergoes a first-order structural phase transition at about 310 K (Smolenskii *et al* 1961). The phase transition separates a high-temperature cubic phase ($Fm\bar{3}m$) from a lower temperature orthorhombic one ($Pnam$). In a recent article (Baldinozzi *et al* 1995) the structure of this compound has been determined in both phases. In the cubic phase, lead and oxygen atoms do not lie on their special positions of the ideal perovskite structure. This seems to be typical of a large number of perovskite compounds. Similar conclusions are proposed for $BaTiO_3$ (Itoh *et al* 1985), $PbMg_{1/3}Nb_{2/3}O_3$ (Verbaere *et al* 1992), Pb_2CoWO_6 (Baldinozzi *et al* 1992). It should be remarked that the orthorhombic phase does not correspond to a simple ordering of the higher-temperature phase.

The present paper is devoted to an experimental study of the phase transition by Raman scattering experiments in order to determine the mechanism of the transition. The modes analysis shows that the atomic displacements can be described as the sum of modulations associated with the wavevectors $q_\Sigma \equiv (\pi/a,\pi/a,0)$ and $q_X \equiv (0,0,2\pi/a)$. The transition mechanism seems to be essentially of displacive nature though an order–disorder contribution should also be present near the transition.

2. Experimental details

2.1. Sample preparation

Powdered samples of Pb_2MgWO_6 have been obtained, starting from stoichiometric amounts of PbO, MgO and WO_3. The solid-state reaction takes place in the three following steps:

§ Now actually at Laboratoire CRISMAT, URA CNRS 1318, ISMRA, F-14050 Caen Cédex, France.

0953-8984/95/428109+09$19.50

heating at 1100 K for 36 hours, grinding and a final heating at 1230 K for 48 hours. Great care was taken to avoid PbO losses. The analysis of powders by x-ray diffraction did not show any trace of the starting products or of parasitic phases.

2.2. Raman scattering

The Raman spectra have been recorded on a Dilor Z24 triple-monochromator instrument equipped for detection with cooled photomultipliers coupled with a counting system. The 514.5 nm emission line of argon ion laser (3 W) has been used. The spectral slit widths were typically 2 cm^{-1}. Low-temperature measurement down to 123 K and high-temperature ones (up to 523 K) were made using a modified sample holder. Temperature regulation was better than ± 1 K.

3. Group theory

3.1. The cubic phase

The classical factor group analysis in the cubic phase for this complex perovskite compound gives the following decomposition onto the zone-centre ($k_0 = \mathbf{0}$) irreducible representations (IR):

$$\Gamma(k_0) = A_{1g} \oplus E_g \oplus T_{1g} \oplus 2T_{2g} \oplus 5T_{1u} \oplus T_{2u}.$$

The cubic phase of Pb_2MgWO_6 may have up to four Raman-active modes (A_{1g}, E_g and T_{2g}) and four infrared-active ones (T_{1u}). The A_{1g} mode is the totally symmetric stretching mode of the octahedra. The E_g mode is also a degenerate stretching mode affecting oxygen octahedra. The T_{1g} mode (which is not optically active) is triply degenerate and corresponds to an octahedra tilt. Both T_{2g} modes are triply degenerate and of bending type. The decomposition also includes *ungerade* modes: one of the five T_{1u} modes has zero frequency and it represents the zone centre acoustic modes. Finally, the modes belonging to T_{2u} IR are not optically active.

Liegeois-Duyckaerts and Tarte (1974) have studied Raman spectra of complex ordered perovskites having a cubic phase at room temperature. They have determined that only oxygen atoms can move in A_{1g} and E_g modes. Oxygen atoms vibrate along W–O–Mg directions and the frequencies of these modes are mainly affected by the strength of W–O and Mg–O bonds. Lead atoms contribute to T_{2g} modes while W and Mg atoms are always at rest.

3.2. Compatibility relations and normal coordinates

Four points of the face-centred-cubic Brillouin zone (figure 1) become zone-centre points in the orthorhombic phase of Pb_2MgWO_6. The space group of the low-temperature phase is *Pnam* (D_{2h}^{16}). Within this conventional setting, the phase transition may be associated with a condensation of modes on the Σ line at $k_4 \equiv (\pi/a,\pi/a,0)$ and at the X point $k_{10} \equiv (0,0,2\pi/a)$ of the Brillouin cubic zone (we have employed Kovalev (1965) notation). The factor group analysis at k_{10} and k_4 gives the following decomposition:

$$\Gamma(k_{10}) = 3X_1 \oplus X_3 \oplus 4X_4 \oplus X_5 \oplus X_6 \oplus X_7 \oplus X_8 \oplus 3X_9 \oplus 6X_{10}$$
$$\Gamma(k_4) = 10\Sigma_1 \oplus 4\Sigma_2 \oplus 8\Sigma_3 \oplus 8\Sigma_4.$$

The orthorhombic phase of Pb_2MgWO_6 has 120 vibration modes. The compatibility relations of the two phases are presented in table 1. The modes A_g, B_{1g}, B_{2g} and B_{3g}

can be Raman-active in the low-temperature phase. We should notice that the modes X_{10} and Σ_3 become totally symmetric (A_g) in the orthorhombic phase.

Table 1. Compatibility relations between the IR associated with the vibrational modes in the cubic and the orthorhombic phase of Pb_2MgWO_6.

$\Gamma \longrightarrow \Gamma$		$X \longrightarrow \Gamma$		$\Sigma \longrightarrow \Gamma$	
$Fm\bar{3}m$	$Pnam$	$Fm\bar{3}m$	$Pnam$	$Fm\bar{3}m$	$Pnam$
$1A_{1g}$	$4A_g$	$6X_{10}$	$6A_g$	$10\,\Sigma_1$	$8A_g$
$1E_g$	$2B_{1g}$	$4X_4$	$6B_{1g}$		$10B_{1g}$
$1T_{1g}$	$3B_{2g}$	$1X_0$	$5B_{2g}$		$4B_{2g}$
$2T_{2g}$	$3B_{3g}$	$0X_2$	$1B_{3g}$	$4\Sigma_2$	$8B_{3g}$
		$1X_8$			
		$3X_9$			
	$1A_u$	$1X_3$	$3A_u$	$8\Sigma_3$	$8A_u$
$5T_{1u}$	$5B_{1u}$	$1X_5$	$3B_{1u}$		$4B_{1u}$
$1T_{2u}$	$6B_{2u}$	$3X_1$	$2B_{2u}$		$10B_{2u}$
	$6B_{3u}$	$1X_7$	$4B_{3u}$	$8\Sigma_4$	$8B_{3u}$

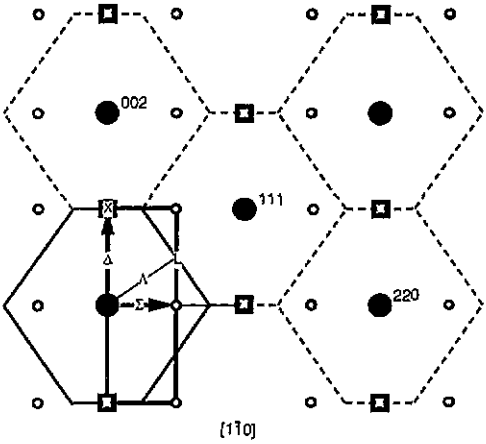

Figure 1. The section of the reciprocal lattice presented here is normal to $[1\bar{1}0]_c$. The orthorhombic reflections represented as squares arise from an X wavevector while those represented as small circles arise from a Σ wavevector. The reflections represented as large full circles (and here indexed as cubic reflections) are the only ones observed in the cubic phase.

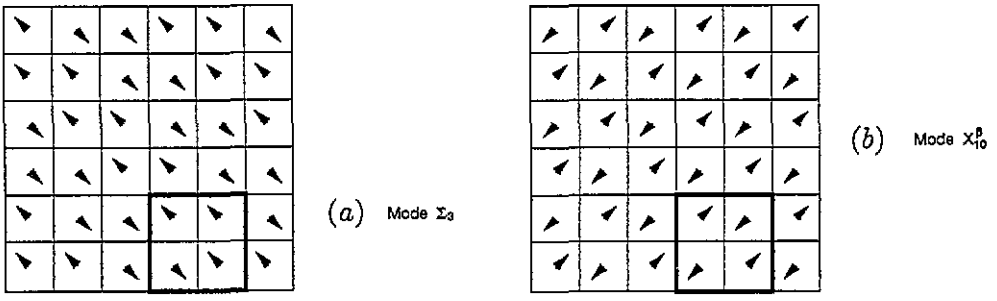

Figure 2. Atomic displacements of lead atoms at $x = 1/a$ associated with the modes Σ_3 (a) and X_{10} (b) which become totally symmetric in the low-temperature phase. Lead atoms vibrate along $[011]_c$.

In table 2 we have represented the symmetrical coordinates of all the off-zone centre modes of the cubic phase which become totally symmetric in the orthorhombic phase. It is interesting to remark that no component along the z-axis is present. Tungsten, magnesium, lead (figure 2) and oxygen atoms O_1 and O_2 vibrate along $\langle 110 \rangle_c$ directions. The vibrations of the others oxygen atoms lie in the (x, y)-plane but they may not belong to a particular direction in this plane.

Table 2. Normal coordinates of off-zone-centre modes which become totally symmetric in the orthorhombic phase.

Atom	X^{α}_{10}	X^{β}_{10}	Σ_3
	α_{10}	α_{10}	α_3
W	$-\alpha_{10}$	α_{10}	$-\alpha_3$
	0	0	0
	β_{10}	β_{10}	β_3
Mg	$-\beta_{10}$	β_{10}	$-\beta_3$
	0	0	0
	γ_{10}	$-\gamma_{10}$	γ_3
Pb_1	$-\gamma_{10}$	$-\gamma_{10}$	$-\gamma_3$
	0	0	0
	γ_{10}	$-\gamma_{10}$	γ_3
Pb_2	$-\gamma_{10}$	$-\gamma_{10}$	$-\gamma_3$
	0	0	0
	δ_{10}	δ_{10}	δ_3
O_1	$-\delta_{10}$	δ_{10}	$-\delta_3$
	0	0	0
	δ_{10}	δ_{10}	δ_3
O_2	$-\delta_{10}$	δ_{10}	$-\delta_3$
	0	0	0
	ϵ_{10}	ϵ_{10}	ϵ_3
O_3	η_{10}	η_{10}	η_3
	0	0	0
	$-\eta_{10}$	$-\eta_{10}$	$-\eta_3$
O_4	$-\epsilon_{10}$	$-\epsilon_{10}$	$-\epsilon_3$
	0	0	0
	$-\epsilon_{10}$	ϵ_{10}	ζ_3
O_5	$-\eta_{10}$	η_{10}	θ_3
	0	0	0
	η_{10}	$-\eta_{10}$	$-\theta_3$
O_6	ϵ_{10}	$-\epsilon_{10}$	$-\zeta_3$
	0	0	0

4. Results and discussion

4.1. Thermal evolution of the spectra

The Raman spectrum recorded in the cubic phase of Pb_2MgWO_6 and presented in figure 3 shows only three sharp peaks (table 3). The assignment of these peaks is straightforward owing to group theoretical predictions and to the previous work of Liegeois-Duyckaerts and Tarte (1974). The three frequencies observed on the Raman spectrum correspond to A_{1g},

$T_{2g}(1)$ and $T_{2g}(2)$ modes. Actually, the E_g peak seems to be systematically absent in all tungstate compounds (Liegeois-Duyckaerts and Tarte 1974).

Table 3. Raman frequencies (cm^{-1}) of Pb_2MgWO_6 at 313 K.

	A_{1g}	E_g	$T_{2g}(1)$	$T_{2g}(2)$
$\bar{\nu}$ (cm^{-1})	844	Not observed	389	64

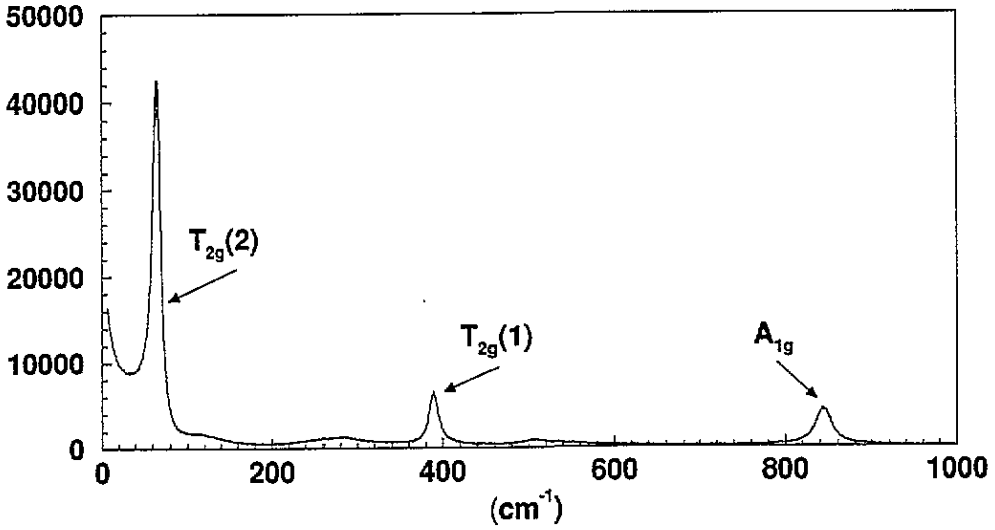

Figure 3. The Raman spectrum of the cubic phase of Pb_2MgWO_6 at 313 K. The main peaks correspond to A_{1g}, $T_{2g}(1)$ and $T_{2g}(2)$ modes. At this temperature, very near to the phase transition, it is easy to observe the modulation of the background.

A series of Raman spectra have been collected at different temperatures ranging between 173 K and 523 K (figure 4). This compound presents a phase transition involving fairly large atomic displacements about the equilibrium positions of the high-symmetry phase (Baldinozzi *et al* 1995). In this case, according to the analysis of Bismayer *et al* (1989), the ordering process will not be simply accompanied by a critical mode softening, but hard modes should also show marked changes in their scattering profiles. These changes are related to the mechanism involved in the structural phase transition.

In the present case, no significant softening or change in the frequencies of the three peaks mentioned above between the transition temperature (310 K) and 523 K, has been observed. On the other hand, the linewidths ($\Delta\bar{\nu}$) of Raman peaks present different evolutions versus temperature. While $\Delta\bar{\nu}$ of A_{1g} and $T_{2g}(1)$ peaks linearly decreases with decreasing temperature, near the phase transition the linewidth of the $T_{2g}(2)$ peak (the low-frequency one) grows a lot (figure 5). This peak does not possess the monotonic evolution of linewidth of the others and is very sensitive to the phase transition: it presents a hard-mode behaviour. It seems reasonable to suppose that the zone centre $T_{2g}(2)$ mode does not play a neutral role in the transition mechanism.

In the orthorhombic phase the splitting of T_{2g} peaks into three components is observed, as expected from the group theory scheme; moreover, it should be remarked that the frequency splitting in this phase is weakly temperature dependent. This behaviour may

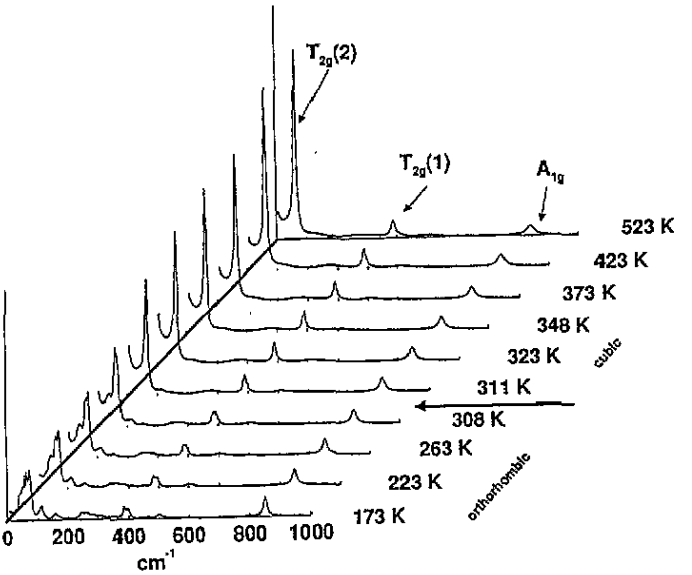

Figure 4. A selection of the Raman spectra collected between 173 and 523 K showing the thermal evolution of the scattered intensities.

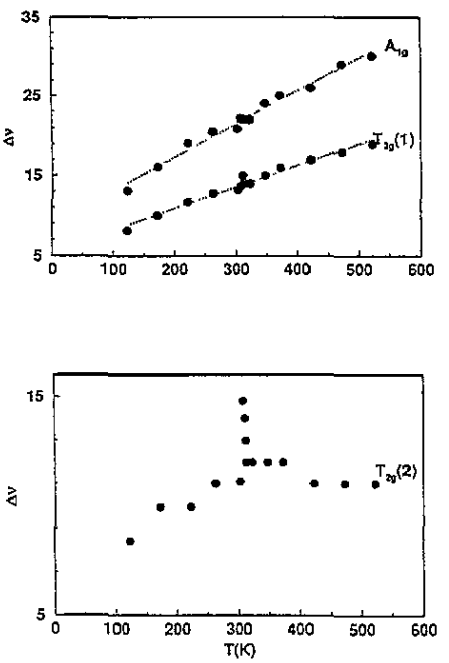

Figure 5. Thermal evolution of the linewidths of A_{1g}, $T_{2g}(1)$ (*a*) and $T_{2g}(2)$ peaks (*b*). The linewidth of the $T_{2g}(2)$ peak is very sensitive of the phase transition. On the other hand the two other peaks present a monotonic behaviour throughout the whole range of temperatures.

be related to a weak anharmonic coupling between elastic strain and the mode components having the same symmetry. Owing to atomic displacements associated with the $T_{2g}(1)$ mode, the observed frequency splitting may give a measure of the internal distortion of

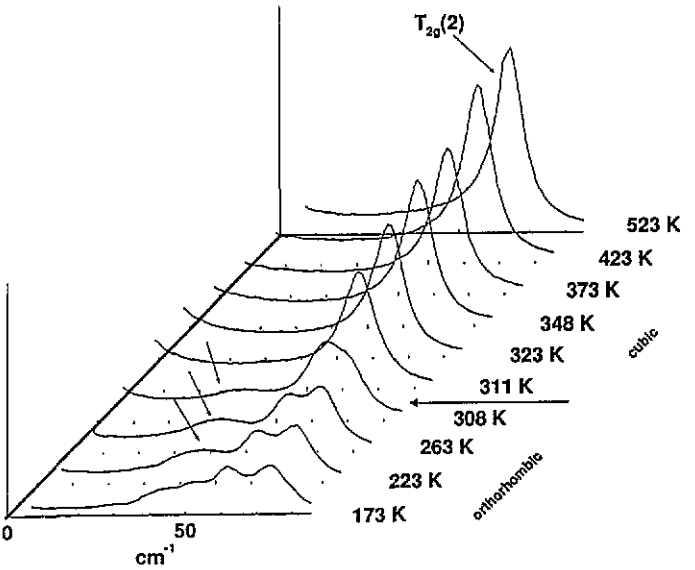

Figure 6. Detail of the low-frequency Raman spectra showing the existence of a soft mode.

octahedra (Rodriguez *et al* 1990).

In the low-temperature phase, we also observe a significant hardening of a peak as temperature is lowered (figure 6). This gives evidence of a displacive character of this transition. This mode is overdamped near the transition and overlaps with the other low-frequency peaks at lower temperatures, so it was not possible to determine a quantitative evolution of the frequency shift.

Finally, it should be noted that the background presents some modulations in the cubic phase. Such broad signals do not correspond to any Raman line allowed by the selection rules in the cubic symmetry of this phase. The amplitude of these modulations increases when approaching the transition temperature from above. In the low-temperature phase these anomalies have stronger intensities, and, as temperature is lowered, they appear structured: in fact, at low temperature, where the linewidths are thinner, it is possible to resolve this broad signal into a several single lines. This phenomenon might be related to precursor effects coming from an orientational disorder affecting oxygen octahedra in the cubic phase (Baldinozzi *et al* 1995).

4.2. Possible transition mechanism

Thanks to the experimental evidence of the displacive character of the phase transition, we may try to explain the orthorhombic phase by a mode condensation. We can show by simple considerations that at least two modes should condense at the phase transition. The analysis of x-ray and neutron diffraction patterns of the orthorhombic phase allows us to operate a classification of superlattice reflections into two families. In fact:

(i) all superstructure reflections may be associated with a single wavevector $q_\Sigma \equiv k_4$;

(ii) but in this case, second-order reflections are much stronger than first-order ones;

(iii) therefore, it is necessary to consider a second wavevector $q_X \equiv k_{10}$ which will generate new first-order reflections in correspondence with second-order reflections generated by q_Σ.

On the other hand, the classical group analysis has showed that the modes X_{10} and Σ_3 become totally symmetric in the orthorhombic phase. These modes condense at the boundary of the Brillouin zone at k_{10} and inside the Brillouin zone at k_4. As for the above-mentioned analysis of diffraction patterns, some further considerations point to a condensation of two modes, as detailed below.

(i) Each of the two modes considered alone (X^{β}_{10} or Σ_3) cannot fully describe the atomic displacements determined by x-ray and neutron diffraction (Baldinozzi *et al* 1995). For instance, the atomic displacement of lead atoms determined by x-ray and neutron diffraction in the orthorhombic phase are along $[100]_c$ or $[010]_c$ while the displacements associated with each one of the two modes are along $\langle 110\rangle_c$ directions.

(ii) To get a fully coherent description of atomic displacement it is necessary to consider the condensation of both modes with equal amplitudes (i.e. leading to the same amplitude of displacements for the lead atoms). In this way, the superposition of the two modes explains all atomic displacements already determined by the diffraction study (figure 7).

(ii) In addition, the interpretation of this atomic displacement with the lattice dynamics approach may explain why the displacements of lead atoms along $[001]_o$ are very small. This displacement is allowed in D^{16}_{2h} but none of the modes that condense involve it, i.e. it results from a coupling with a secondary order parameter.

The description of the orthorhombic phase given by the diffraction study and the one given by the group analysis are coherent and they fully explain the reasons for the atomic displacements determined.

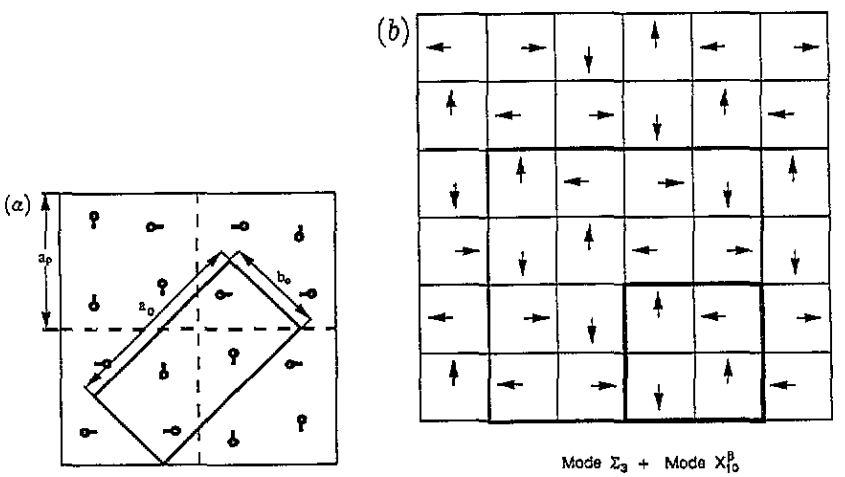

Figure 7. (*a*) Atomic displacements of lead atoms at $x = 1/a$ determined by structural study (Baldinozzi *et al* 1995). (*b*) The corresponding displacements resulting from the superimposition of the X^{β}_{10} and Σ_3 modes.

4.3. Application to Pb_2CoWO_6

The transition mechanism outlined above should be extended to another complex perovskite-type compound, Pb_2CoWO_6. The phase transition sequence (Brixel *et al* 1985) of this compound is rather complex (phase I cubic, phase II monoclinic incommensurate, phase III orthorhombic as in Pb_2MgWO_6). The high-temperature phase ($Fm\bar{3}m$) and the lower-temperature one ($Pnam$ or $Pna2_1$) are very close to those of Pb_2MgWO_6. If a direct

transition $Fm\bar{3}m$ to $Pnam$ is considered, the same transition mechanism can be proposed. In fact, a recent study by convergent beam electron diffraction (Baldinozzi *et al* 1994) suggests that no displacement of lead atoms exists along $[001]_o$. In this case the same modes can be involved in the transition mechanism. On the other hand, if the orthorhombic phase is $Pna2_1$ two additional modes condense (X_9 and Σ_4). The condensation of X_9^{β} and Σ_3 will lead to a non-centrosymmetric structure where the atoms may present displacements along $[001]_o$.

4.4. Conclusions

The Raman scattering studies of Pb_2MgWO_6 reveal the existence of a soft mode in the low-temperature phase which unambiguously proves the existence of a displacive character for the cubic–orthorhombic phase transition; since such softening is not observed in the cubic phase, one can conclude that the mode that condenses is a off-zone-centre mode. Actually, both the diffraction results and the group theory analysis show that the transition can be explained by the condensation of X_{10}^{β} and Σ_3 modes. Presumably, one of these modes condenses, while the freezing-in of the other one is induced by some coupling. On the other hand, the existence of unexpected diffuse Raman signal in the cubic phase indicates for the existence of some order disorder contribution too.

References

Baldinozzi G, Sciau P and Lapasset J 1992 *Phys. Status Solidi* a **133** 17

Baldinozzi G, Sciau P, Pinot M and Grebille D 1995 *Acta Crystallogr.* B **51** at press

Baldinozzi G, Sciau P, Buffoot P A and Stadelmann P 1994 *Electron Microsc.* **1** 875

Bismayer U, Devarajan V and Groves P 1989 *J. Phys.: Condens. Matter* **1** 6977

Brixel W, Werk M L, Fischer P, Buhrer W, Rivera J P, Tissot P and Schmid H 1985 *Japan J Appl. Phys. Suppl.* 2 **24** 242

Itoh K, Zeng L, Nakamura E and Mishima N 1985 *Ferroelectrics* **63** 29

Kovalev O V 1965 *Irreducible Representations of the Space Groups* (New York: Gordon and Breach)

Liegeois-Duyckaerts M and Tarte P 1974 *Spectrochim. Acta* A **30** 1771

Rodriguez V, Couzi M, Tressaud A, Grannec J, Chaminade J P and Ecolivet C 1990 *J. Phys.: Condens. Matter* **2** 7387

Smolenskii G A, Krainik N N and Agranovskaya A I 1961 *Fiz. Tverd. Tela* **3** 981

Verbaere A, Piffard Y, Yé Z G and Husson E 1992 *Mater Res. Bull.* **27** 1927